Osteo mineralization of fibrin-decorated graphene oxide Original Research Article Carbon, In Press, Corrected Proof, Available online 5 January 2013 R. Deepachitra, M. Chamundeeswa...

ARTICLE *in* CARBON

Impact Factor: 6.2

READS

43

7 AUTHORS, INCLUDING:

Baskar Santhosh Kumar

Council of Scientific and Industrial Researc...

28 PUBLICATIONS **23** CITATIONS

SEE PROFILE

Thotapalli P Sastry

Central Leather Research Institute

96 PUBLICATIONS **767** CITATIONS

SEE PROFILE

CARBON 56 (2013) 64–76

Available at www.sciencedirect.com

SciVerse ScienceDirect

journal homepage: www.elsevier.com/locate/carbon

Osteo mineralization of fibrin-decorated graphene oxide

R. Deepachitra [a], M. Chamundeeswari [b], B. Santhosh kumar [a], G. Krithiga [a], P. Prabu [a], M. Pandima Devi [c], Thotapalli P. Sastry [a,*]

[a] Bio-Products Laboratory, Central Leather Research Institute, Adyar, Chennai 600020, India
[b] St. Joseph's College of Engineering, Sholinganallur, Chennai 600119, India
[c] Department of Biotechnology, SRM University, Katankulathur, Chennai 603203, India

ARTICLE INFO

Article history:
Received 23 August 2012
Accepted 20 December 2012
Available online 5 January 2013

ABSTRACT

Surface functionalized graphene oxide (GO) was synthesized by coating fibrin on its surface. The fibrin coated graphene oxide (FGO) was characterized for its physiochemical properties and its potential as an osteoinductive material was evaluated using osteoblast like cell line MG-63 and normal cell line NIH 3T3. The scanning electron microscopy (SEM) has confirmed the coating of fibrin on GO and the transmission electron microscopy (TEM) revealed both spherical and cubical nature of GO nanoparticles and FGO. In *in vitro* studies, FGO exhibited higher levels of alkaline phosphatase and calcium ion release which confirmed the osteoinductive nature of FGO. The 3-(4,5-dimethylthiazol-2-Y)-2,5-diphenyltetrazolium bromide (MTT) assay proved FGO as a biocompatible material. The results have suggested that FGO might be a promising scaffold for bone tissue engineering applications.

1. Introduction

Graphene is a two dimensional, sp^2 hybridized material having very interesting electronic, thermal, and mechanical properties. It has also been used as a biomaterial for various biomedical applications such as biosensors, biomedicine, bio-imaging, drug delivery and biodetection etc. [1,2]. The *in vivo* and *in vitro* biological studies of graphene oxide (GO) give an idea about the biocompatibility of GO, which can be used as a scaffold for cell culture studies [3,4]. The GO materials are strongly dispersed in water; the hydrophilicity is due to the presence of hydroxyl, carbonyl and epoxy groups on the surface. These functional groups are present on the basal plane and edges of GO enables greater interactions with proteins through covalent, electrostatic and hydrogen bonding [5,6]. The flat monolayers of carbon atoms are closely packed into a two-dimensional honeycomb crystal structure perform as a platform for the addition of various biomolecules, which form the incredible GO-biomaterials. The graphene biomolecules are used in different fields for various applications.

The surface functionalized graphene based nanomaterials are quite interested in biological studies. The surface modifications can be affected by the integration of nucleic acids, proteins, peptides and sometimes with cells also. The biologically modified graphene compound shows good biocompatibility, solubility and selectivity, that's why most of the studies are focused on graphene modification and functionalization [7,8]. Proper surface modification is very important for the application of GO composites in biological systems.

Fibrin (F) is an insoluble protein, serves as an ideal substrate for cell attachment, proliferation, extracellular matrix formation in wound healing. It is used as a biological scaffold in tissue engineering. Fibrin has been extensively used in the form of sponge, glue and microbeads because of its good biocompatible and biodegradable properties. Drugs can also be coupled to the fibrin based nanomaterials through the ligand [9–11]. In the present study crude fibrin which is a major solid waste in Indian slaughter houses is used as a starting material for the preparation of pure fibrin. The preparation of pure fibrin from its crude counterpart is described elsewhere

* *Corresponding author:* Fax: +91 44 24912150.
E-mail address: sastrytp@hotmail.com (T.P. Sastry).
0008-6223/$ - see front matter
http://dx.doi.org/10.1016/j.carbon.2012.12.070

[12,13]. Fibrin has played a vital role in orthopedic surgery in the form of sealant [14], glue [15], or adhesive [16] to enhance osteogenesis. Fibrin is also expected to act as an angiogenic factor, can increase cell retention, which will have a significant role in promoting early differentiation of osteogenic cells [17]. The fibrin glue can be used as tissue engineering scaffold because of its non-inhibition of cell morphology, growth, proliferation and differentiation [18].

Osteoblastic cell lines like MG-63, SaOS-2, U-2OS, and CPC-2 are derived from human osteosarcoma bone cell lines. These cell lines contain important markers of osteogenic cell differentiation, such as the activity of ALP and production of bone growth factors [19].

The novelty of the present work lies in the surface modification of graphene oxide by coating the fibrin on its surface. The attachment of fibrin on the surface of GO may be due to the interaction of amino groups of fibrin with the carboxyl groups on the surface of GO through electrostatic, π–π and hydrophobic interactions. The main aim of the present study is to find out the efficacy of FGO as an osteoinductive material.

2. Experimental section

2.1. Materials

Graphite powder was obtained from Lobo Chemicals, India. The fibrin was collected form Municipal Corporation slaughter house, Chennai, India. The MG-63 and NIH 3T3 cell lines were collected from National Centre for Cell Science (NCCS), Pune, India. The 10% bovine serum, Dulbecco's minimal eagles medium (DMEM), antibiotics and Alizarin Red Dye were obtained from HiMedia, India.

2.2. Preparation of graphene oxide surface decorated by fibrin

Graphite oxide was prepared from Graphite (G) by Hummers method [20]. Briefly 100 mg of graphite oxide powder was dispersed well in 100 ml of water, and it was sonicated by using probe sonicator for 30 min under room temperature and 25% amplitude. The homogeneous colloidal suspension of graphene oxide was occurred. The concentration of GO was obtained as 1 mg/ml, this GO suspension was stored for further studies.

The crude fibrin was collected from the slaughter house and washed thoroughly under running water to remove the blood clots. The fibrin was treated with 0.5 M sodium acetate solution and 30% hydrogen peroxide solution, later fibrin was washed thoroughly under running water and made into a paste using a domestic mixer. The solid content of the final purified fibrin was around 40%.

The purified fibrin was dissolved in 1 N NaOH solution, and was added drop by drop to the acidified GO solution (pH-1) under vigorous stirring (1500 rpm). At pH 6–6.5 fibrin was coated onto GO particles, this is visualized as the brown color GO solution turns into turbid white solution. This FGO solution was used to evaluate osteoinductive properties using MG-63 cell line. The formation of the fibrin decorated graphene oxide (FGO) and its osteoblastic cell attachment is schematically represented in Fig. 1.

2.3. Characterization

The UV–Visible absorption spectra for the samples were measured with JASCO UV–vis spectrophotometer (Model: V570 UV–vis–NIR). The samples were placed in a 1 cm quartz cell.

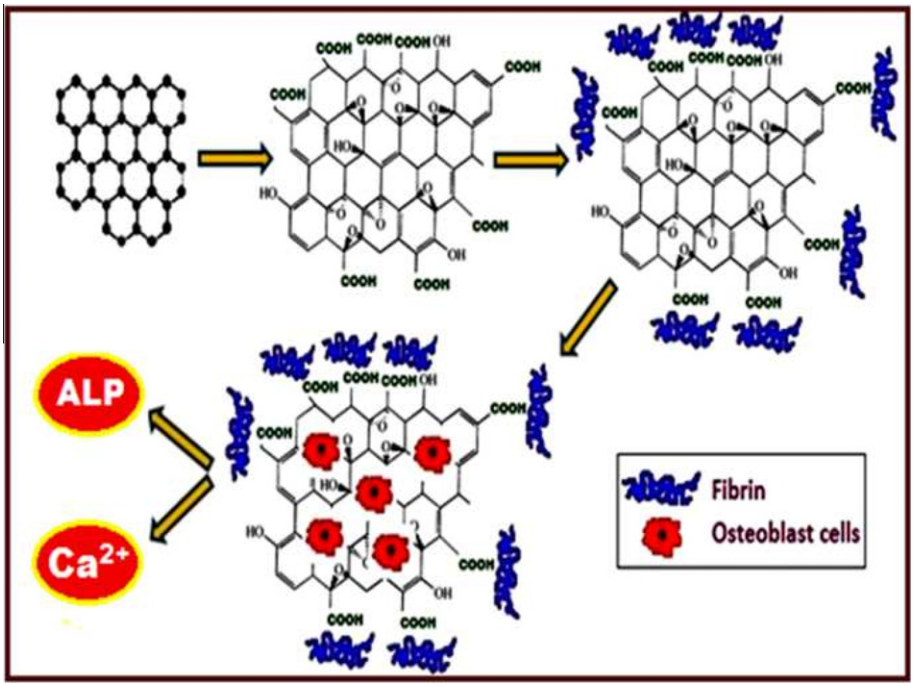

Fig. 1 – Graphical representation of fibrin decorated graphene oxide as an osteomaterial.

The X-ray powder Diffraction (XRD) patterns were done with Seifert JSO Debyeflex 2002. X-ray Diffractometer (30 mA, 40 kV) using Cu Ka radiation (k = 0.154056 nm). The IR spectrum is performed with a Nicolet Impact 400 Fourier-Transform Infrared (FTIR) spectrophotometer to confirm the surface functional groups of the G, F, GO and FGO. Powder samples were mixed with anhydrous potassium bromide (KBr), pelletized, and used for FT-IR analysis. The model of the Atomic force microscopy (AFM) is Agilent Pico LE Scanning Probe Microscope. The Agilent instrument is a tip scan instrument, equipped with small (10 μm) and large AFM scanners (150 μm). This instrument is equipped with an environmental chamber, is capable of heating to 200 °C. The surface structure analysis of the samples was visualized by scanning electron microscopy (Hitachi S-4800) attached with Phonix Energy dispersive X-ray spectroscopy (EDX), which was carried out the elemental analysis. The dried and powdered samples were coated with gold ions using ion coater under the following conditions: 0.1 Torr pressure, 20 mA current and 70 s coating time, using a 15 kV accelerates voltage. The Transmission electron microscopy (TEM) analysis was done by TECHNAI-10, PHILIP imported form Netherlands. The 20 μl sample was added with 10 μl of phospho tungstic acid, dried it in a copper coated grid under 37 °C.

2.4. Cell culture study

2.4.1. MTT assay

The MG-63 cells were grown in a 96-well plate in DMEM, supplemented with 10% fetal bovine serum and antibiotics (streptomycin, penicillin-G, kanamycin, amphotericin B). About 25 μl cell suspension ($5x10^3$cells/well) was seeded in all 96 wells and incubated at 37 °C for 48 h in 5% CO_2 for the formation of confluent monolayer. The monolayer of cells in the plate was exposed to various dilutions of drug of interest. The cell viability was measured after 96 h using 3-(4,5-dimethylthiazol-2-Y)-2,5-diphenyltetrazolium bromide (MTT) assay with MTT and 10% dimethyl sulfoxide (DMSO). This tetrazolium salt is metabolically reduced by viable cells to yield a blue insoluble Formazan product, measured at 570 nm spectrophotometrically. Controls were maintained throughout the experiment (untreated wells as cell control and diluents treated wells as diluents control). NIH 3T3 cells were used as a negative control and similar treatment as that of MG 63 was carried out. The assay was performed in triplicates. The antitumor assay was performed using osteoblastic cell lines (MG-63). The assay was performed in triplicates for each of the FGO particles. The concentrations of tested materials are in the range of 25–200 μg/ml, Cyclophasphamide anticancer drug was used as a positive control (PC).

The mean of the cell viability values was compared to the control to determine the effect of the FGO on cells. A graph was plotted against the optical density at 570 nm vs the concentrations of FGO.

2.4.2. Alkaline phosphatase

The Alkaline phosphatase (ALP) effect of FGO was measured in culture supernatants using a procedure which involves a colorimetric assay using p-nitrophenyl phosphate as substrate, and measuring spectrophotometrically the p-nitrophenol released at 405 nm with the absorbance being proportional to the ALP activity. Cells were (MG 63 and NIH 3T3) seeded onto 24 well plates and were treated with the three different concentrations of FGO in 50, 100 and 200 μg/ml concentrations. After different periods of incubation, cell free supernatants were collected for further ALP assay. The determinations were performed using three replicates each time. All the treatments were compared against control wells (cell line with ordinary DMEM without treatments) [21].

2.4.3. Calcium assay

In a biochemical assay, alizarin red is used to determine quantitatively by colorimetric method for the presence of calcium deposition by cells of an osteogenic cell line lineage. The formation of calcium phosphate by MG-63 osteoblast like cells was determined as described by using the alizarin red-S assay. The medium was removed, and the cell layers on the matrix were rinsed with phosphate buffered saline (PBS) three times and fixed in 3.6% (v/v) formaldehyde at room temperature for 15 min. The fixed cells were stained with 2% alizarin red S (pH 4.1–4.3) for 15 min at 25 °C. Then, the cell layers were washed with deionized water for quantification of staining, 800 ml of 10% (v/v) acetic acid was added to each well, and the wells were incubated at room temperature for 30 min with shaking. The cell layers on the wells were lifted and transferred to a 1.5 ml micro centrifuge tube. After vortexing for 30 s, the pellet was overlaid with 50 μg/ml mineral oil, heated to 85 °C for 10 min, and transferred to ice for 5 min. The pellet was centrifuged at 20,000g for 15 min and 50 μg/ml of the supernatant was removed to a new 1.5 ml micro centrifuge tube. Then, 200 μg/ml of 10% (v/v) ammonium hydroxide was added to neutralize the acid. The absorbance of the supernatant was measured in triplicates at 405 nm [22]. Similar study was carried out using NIH 3T3 cells to prove that osteogenesis has occurred only in oseteoblast like cell line and not in the normal cell line.

2.5. Statistical analysis

The statistical analysis data was expressed as the arithmetic mean ± standard deviation with $n = 3$. The results were performed by using multiple t-test. The significant difference level is $p \leqslant 0.05$.

3. Results and discussion

The UV–Vis spectrum of GO (Fig. 2a) shows a maximum absorption (λ_{max}) at 230 nm. This is the characteristic peak of GO layers due to the π–π electron interactions in the polyaromatic ring system [23]. The fibrin λ_{max} is observed at 270 nm in (Fig. 2b) and that of FGO was observed at 275 nm in (Fig. 2c). The shifting in the peak may be due to the interaction of fibrin with GO.

Fig. 3 shows the XRD spectra of the graphite (a), and graphene oxide (b). The graphite XRD shows a narrow peak at d_{002} $2\Theta = 26.3$, the d spacing between the two sheets are 3.37A°. The XRD of GO exhibits a sharp peak at $2\Theta = 10.1^0$, corresponding to the reflection (001) with the interplane distance of $d_{001} = 8.6$. When graphite is oxidized, more oxygen groups are bonded to the planar surface of graphite, forming a sharp

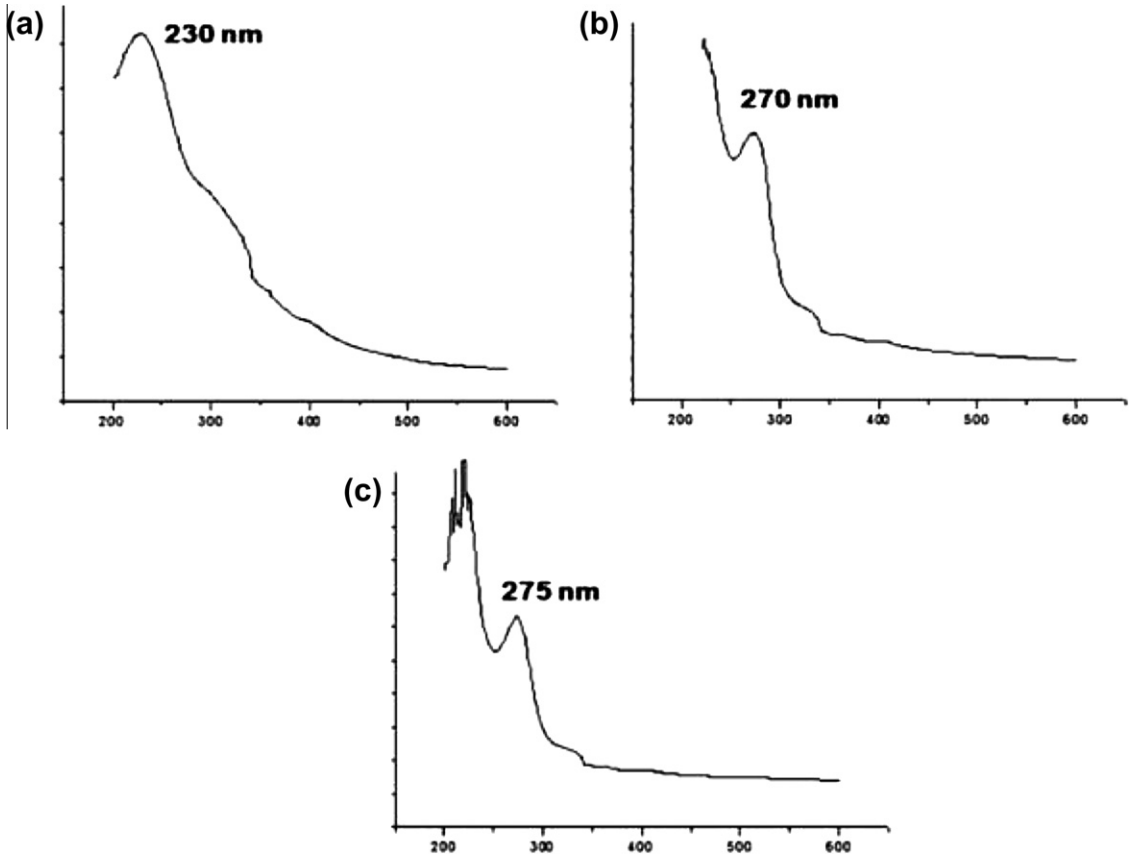

Fig. 2 – UV Visible absorption spectra of GO (a), F (b) and FGO (c).

peak at 10.1^0 [24]. This sharp peak does not occur in the graphite flakes, indicating the formation of GO.

Fig. 4 shows the FT-IR spectra of G (a), GO (b), F(c), and FGO (d). The characteristic vibrations of GO are observed in (Fig. 4b); broad –OH group peak at 3401 cm^{-1}, a C=O stretching vibration peak at 1718 cm^{-1}, a C–OH stretching peak at 1225 cm^{-1} and C–O stretching peak at 1040 cm^{-1} [25]. A peak attributed to the vibrations of un-oxidized graphitic skeletal domains and the adsorbed water molecules at 1620 cm^{-1} was observed, as for graphite, the spectrum is essentially featureless except the C=C conjugation (Fig. 4a). The IR spectrum of FGO (Fig. 4d) shows interaction between –COOH groups available on the surface of GO and the amide groups of the fibrin. This interaction is manifested as the amide I, amide II, amide III peaks in the spectrum of fibrin present at 1656, 1533 and 1241 cm^{-1}, respectively in Fig. 4c and are shifted to 1650, 1577 and 1262 cm^{-1} in the spectrum of FGO. At the same time the prominent band representing –COOH group at 1718 cm^{-1} is almost disappeared and seen as a shoulder at 1742 cm^{-1}. These observations clearly indicate the interaction between the –COOH groups of GO and $–NH_2$ groups available on the backbone of F.

The atomic force microscopic pictures in Fig. 5 illustrate the size and thickness of GO (a) GO and (c) FGO. The chemically exfoliated GO length was found to be in several nanometers to micrometer size. The thickness was found to be in 1.7–2 nm (Fig. 5b), similar results were obtained in previous studies [26,27]. The AFM graph of FGO exhibited the increase in the thickness to 7 nm (Fig. 5d); this may be due to the coating of F onto GO. After the conjugation of biomolecules, surface morphology GO was changed [28].

The surface morphology of GO (Fig. 6a) shows the brittle crystalline structure and the shape of the GO crystals were found to be cubical. The SEM of FGO (Fig. 6b) shows the embedded GO particles in fibrin. The higher magnification of SEM clearly shows the decoration of fibrin on GO crystals. The EDX proves the presence of 55% of carbon atoms and 45% oxygen atoms in GO. The fibrin coated GO shows the 21% of oxygen atoms, 75% of carbon and 8% of nitrogen atoms. The presence of nitrogen indicates the conjugation of fibrin with GO. The TEM analysis of GO (Fig. 7a) shows cubical and spherical nature of GO nanoparticles with the size ranging from 39 to 500 nm. The TEM image of FGO (Fig. 7b) shows the embedding of GO nanoparticles in the fibrin; these results exhibit the coating of fibrin on GO.

The MTT assay of the GO and FGO was carried out using MG-63 (25–200 μg/ml) and NIH 3T3 (25–100 μg/ml) cell lines at different concentrations. The treated cells were incubated for 48 h on MG-63. The three important factors for the cell viabilities are (a) thickness of the material (b) compactness of the cells and (c) Reactive Oxygen Site [24]. Fig. 8a shows cell viability of GO and FGO. The cell viability was calculated using the formula given below.

$$\text{Survival rate of cells}(\%) = A_{570}(\text{sample})/A_{570}(\text{control}) \times 100$$

The biocompatibility at lower concentration clearly shows the cell attachment on the surface of the GO and FGO. A difference in the cell attachment is observed with the increase in

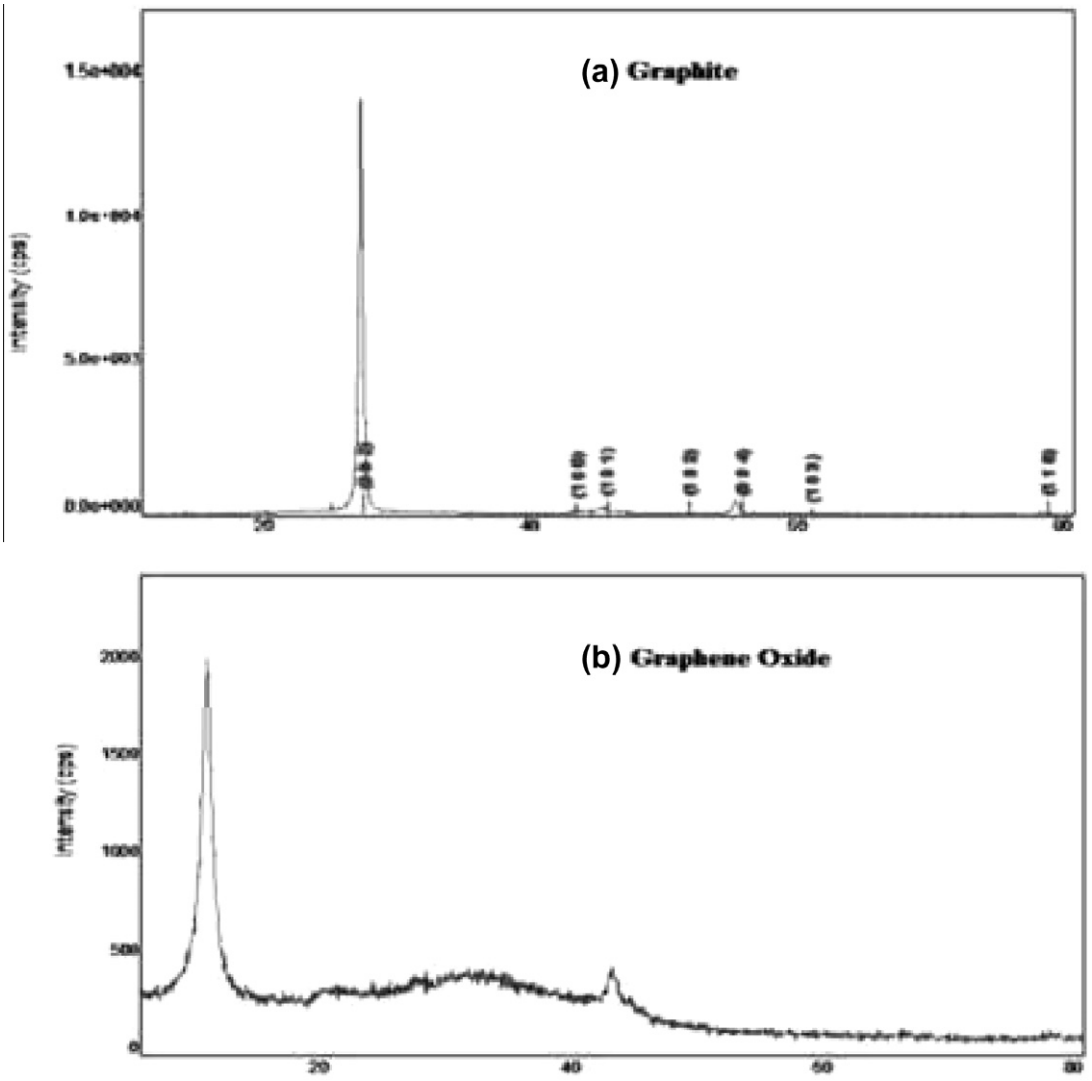

Fig. 3 – XRD spectra of Graphite (a) and Graphene oxide (b).

the dosage of GO and FGO. According to the earlier studies, the sonicated GO particles have a single layer thickness which facilitates the biological studies. The purity of graphene and graphene oxide does not affect the growth of living cells in the biological studies [29].The oxygen functionalized groups(–COOH, –OH, epoxy) on the surface of GO helps the cell attachment, cell viability and cell adhesion due to the increase of polarity and wet ability of GO [30,31]. Biological experiments using GO were held in the adherent cells such as osteoblasts, mesenchymal stromal cells, stem cells etc. The non cytotoxicity studies of GO was carried out previously in various cells such as L929 cells [32], HeLa cells [33], human fibroblasts [24,34], A549 human lung cancer cells [35] and human hepatoma HepG2 cells [36]. Only one atom thickness of GO has the particular properties (elasticity, flexibility, and adaptability) which increases the mechanical strength of GO and induces the cell proliferation, adhesion and differentiation [36,37]. In our study the results were similar with previous studies. The cell viability of GO ranges from 85% to 70% on MG-63.

The surface topography of the FGO is the important aspect for the cell attachment and the viability, since at the lower concentration (25 and 50 μg/ml) FGO has more amounts of surface oxygen groups, which induce the cell attachment. The 100 μg/ml of FGO shows 90% of the cell viability due to the good interaction between the cells and the compound. The decrease in rate of cell viability at 200 μg/ml is due to higher loading of the sample, which might have inhibited the growth of cell adhesion due the Reactive Oxygen Site (ROS) generation. ROS is created by the cleavage of oxygen molecules into free radicals and induce the oxidative stress, inflammation and the structure of enzymes; extracellular matrix molecules and cell membranes were changed. These changes may affect the cell attachment and DNA fragmentation of the cells [19]. ROS is the concentration dependent factor which stimulates the cytotoxicity on the cells. The higher concentration of GO lead to more oxidative stress on cells [35]. This may be due to the aggregation (or) extension of higher loading of the sample inducing the ROS. The surface functionalized GO induces the reduction of hydrophobic interaction as well as ROS.

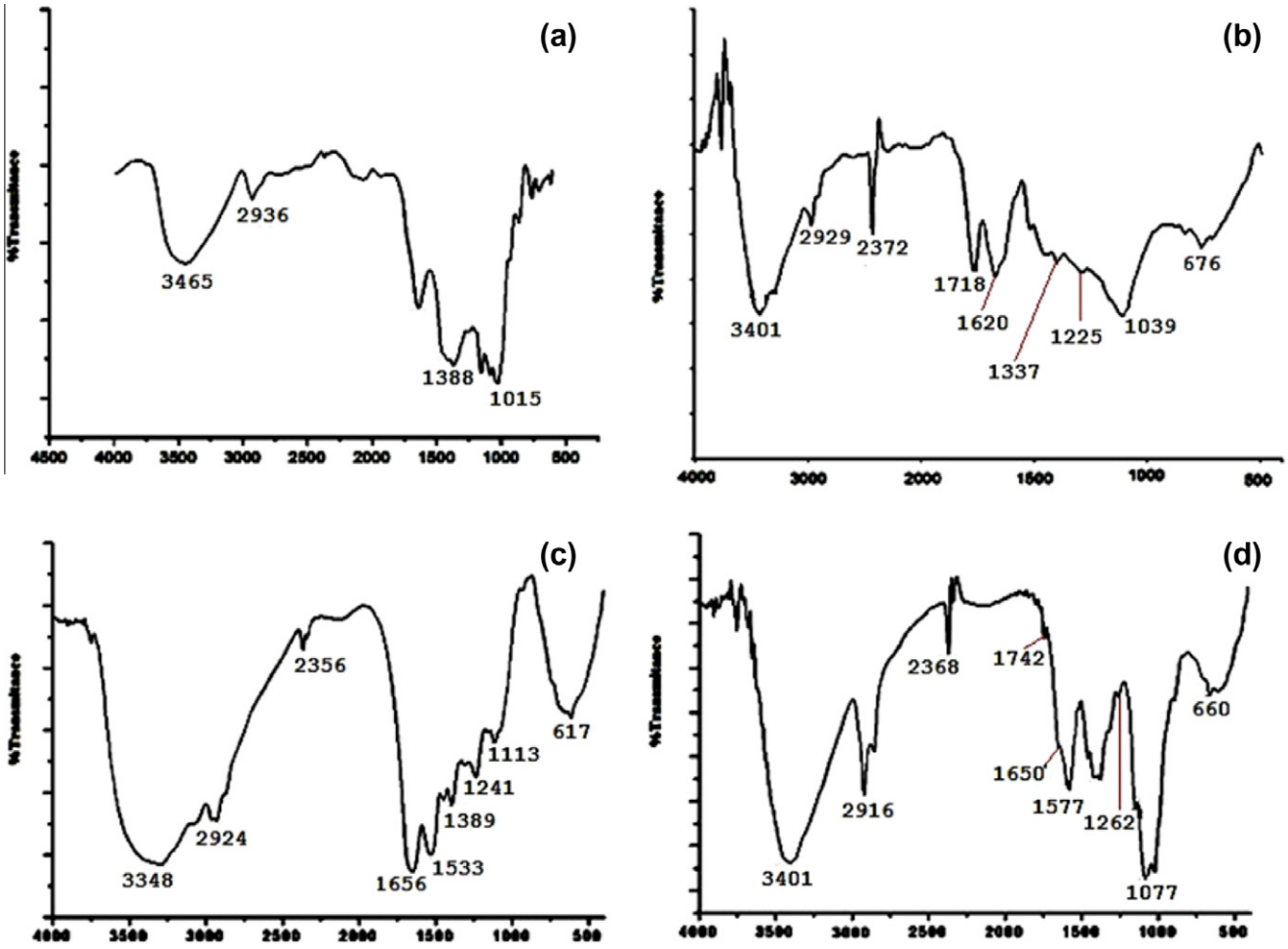

Fig. 4 – Fourier transform infrared spectra of (a) Graphite, (b) Graphene oxide, (c) Fibrin and (d) Fibrin decorated Graphene oxide.

The phase contrast microscopy image shows, the morphological changes of MG-63, with GO and FGO. Oval to spindle-shape cells were observed and not divided separately (Fig. 8b) indicating that the shape of the cells does not change with the increase in concentration, compared with the control. The cell morphology study of GO and FGO materials are independent of the dosage. The FGO exhibit the similar cell density with the control. The fibrin seems to be a good biocompatible compound which does not induce the cytotoxicity, and shows good cell viability even with the higher concentration.

The cell death was studied using an anticancer drug cyclophosphamide as PC; the cells were treated and incubated for 48 h. The survival rate of the cells with PC 200 μg/ml was found to be only 5%, which indicates the serious cell death. When the cells are treated with the same concentration of GO and FGO (200 μg/ml) shows a higher viability rate 70% and 85%, compared with control (100%). This shows that the cell death is considered to be high (5% cell viability) with positive control and the viability rate has increased with the GO and FGO.

The biocompatibility of GO and FGO were studied by using NIH 3T3. This study was held for 4 days. The Fig. 9 shows the cell viability rate after the treatment of GO and FGO. According to our results the FGO shows very good cell attachment and cell proliferation also. The significance difference is occurred at the 100 μg/ml of FGO on 1st day and 25 μg/ml of FGO on 4th day. The cell viability rate of FGO is merely equal to 100% even after 4 days treatment. This again proves the fibrin which reduces the cytotoxicity of GO and improves biocompatibility of GO in cell culture studies. The microscopic image shows the cell morphology after the treatment of GO and FGO of 100 μg/ml on 4th day. The cell density of FGO was similar with control, which strongly indicates the good biocompatibility of FGO.

The ALP is a metalloenzyme, is being used as an osetoinducer in bone formation and a characteristic enzyme for osteoblast differentiation. The role of tissue nonspecific ALP in bone formation is to degrade the inorganic pyrophosphate (Pi-inhibitor of Hydroxyapatite) and generate the inorganic phosphate [28]. The fibrin scaffold is used as Pi modulator for bone formation. The formation of Pi by ALP is the basic requirement for mineralization effect on osteoblast cells, so the ALP study is preliminary one for bone formation in osteoblast.

The Figs. 10 and 11 shows the ALP enzyme levels at three different concentrations (25, 50, 100 μg/ml) on MG-63 and NIH 3T3 cells. The study was carried out at four time intervals

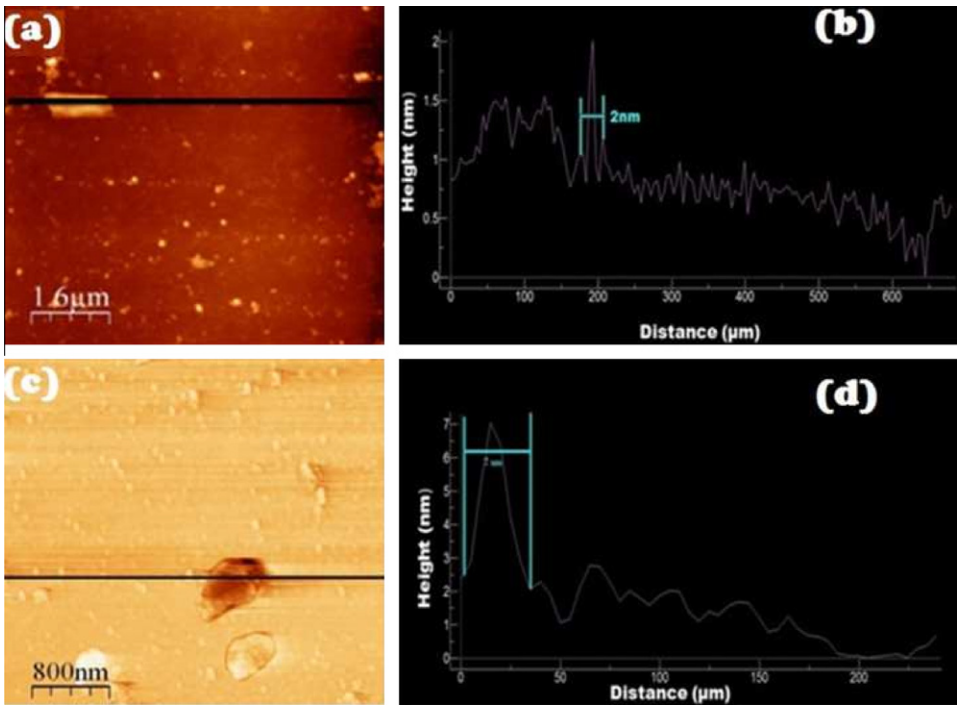

Fig. 5 – AFM image of GO (a), height profile of GO (b), AFM image of FGO (c) and single particle height profile of FGO (d).

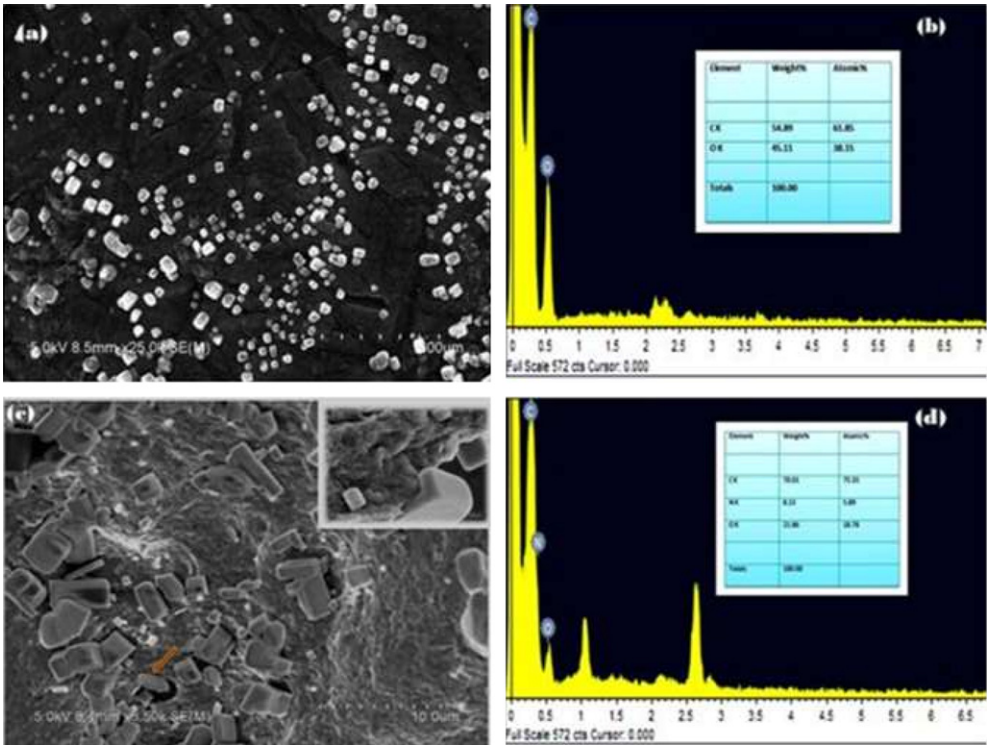

Fig. 6 – Scanning electron microscopic image of GO (a) and energy (EDX) profile of GO (b). SEM image of FGO (c), the inset shows the magnified image of FGO, EDX profile of FGO (d).

(0th day, 4th day, 8th day and 12th day). Among these days, the 12th day exhibited good ALP levels, when compared to that of control. Among all the three concentrations the (25 and 50 μg/ml) of FGO shows the higher ALP level on 12th day. The 100 μg/ml of FGO shows good result on 8th day itself. All the three concentration of FGO induces more ALP level when compared with control. The GO induces lower ALP level compared with FGO. There is no significance difference

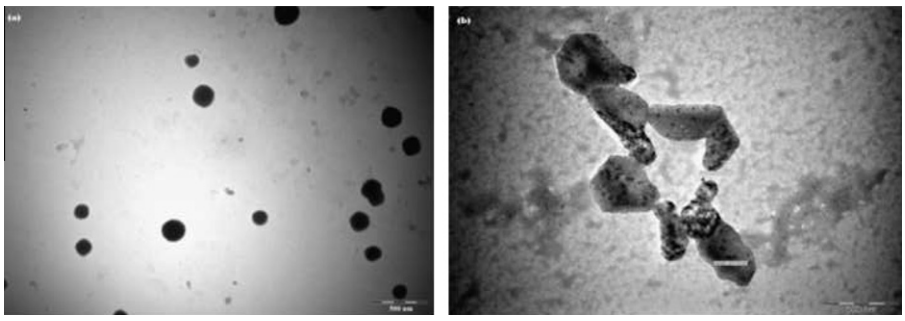

Fig. 7 – Transmission electron microscopic image of GO (a) and FGO (b).

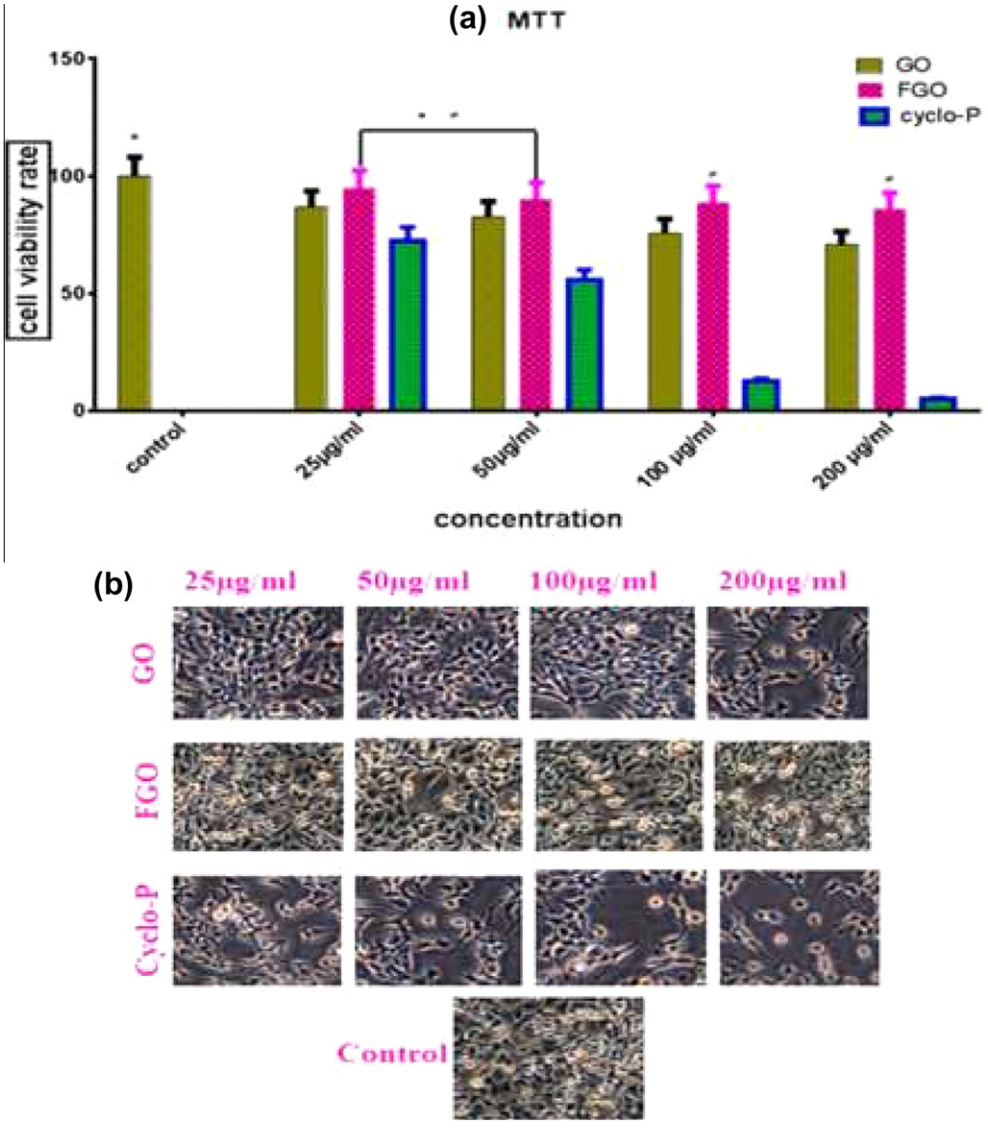

Fig. 8 – MTT Assay representation of GO, FGO, Cyclo-P on MG-63 and cells (a). The microscopic images clearly show the cell death of different concentration (b). Significant difference ($p \leqslant 0.05$) occurred at all the concentration of FGO compared with GO and positive control. The 25 and 50 μg/ml of FGO not have any significant difference with control. The 100 and 200 μg/ml shows the significant difference with control. The significant difference is calculated by using *t*-test.

occurred at GO concentrations. Among these results we can conclude that fibrin is a good osteoinducer. The ALP level was tested on NIH 3T3 cells is used as negative control. There is no any ALP level increase up to 12th day on fibroblast cells for both GO and FGO. This clearly proves the osteoinduction capacity on MG-63.

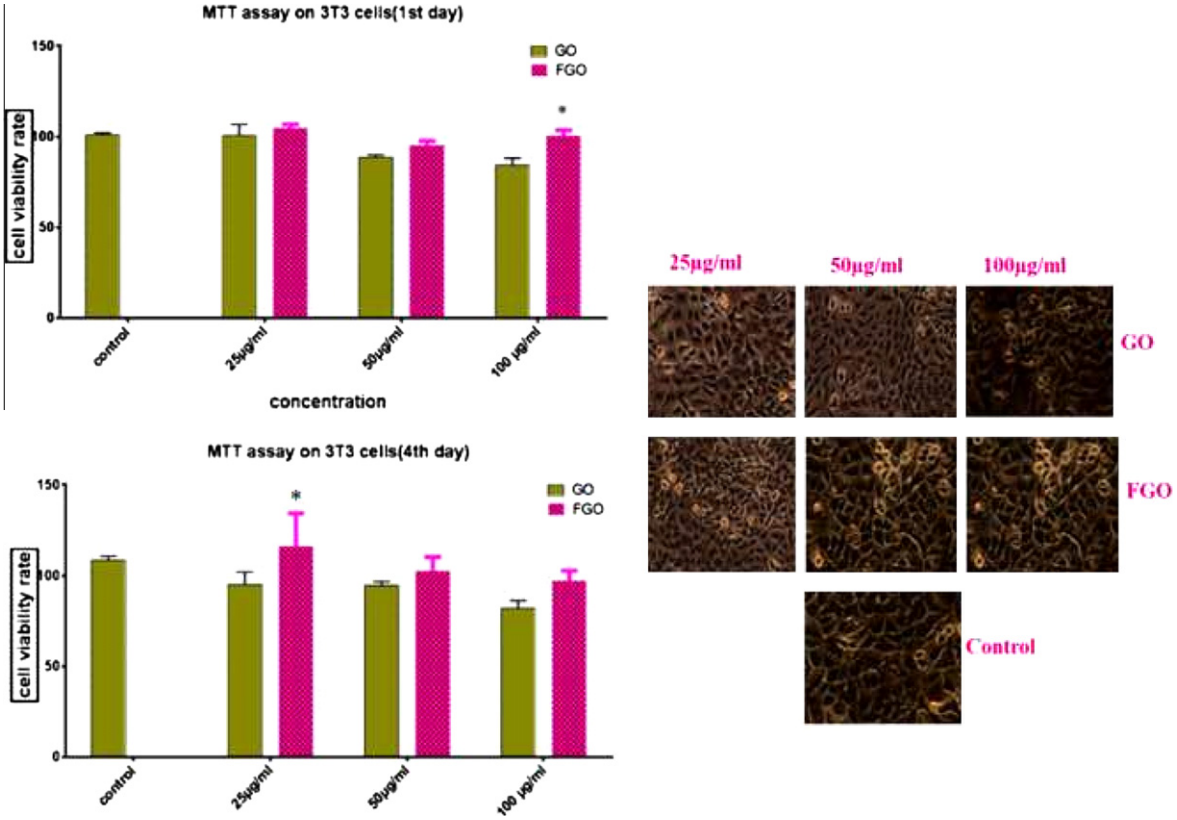

Fig. 9 – MTT Assay representation of GO, FGO on NIH 3T3 cells. The microscopic images clearly show the cell death of different concentration. Significant difference ($p \leqslant 0.05$) occurred at 100 µg/ml concentration of FGO on 1st day, 25 µ/ml FGO on 4th day. The significant difference was calculated by using t-test.

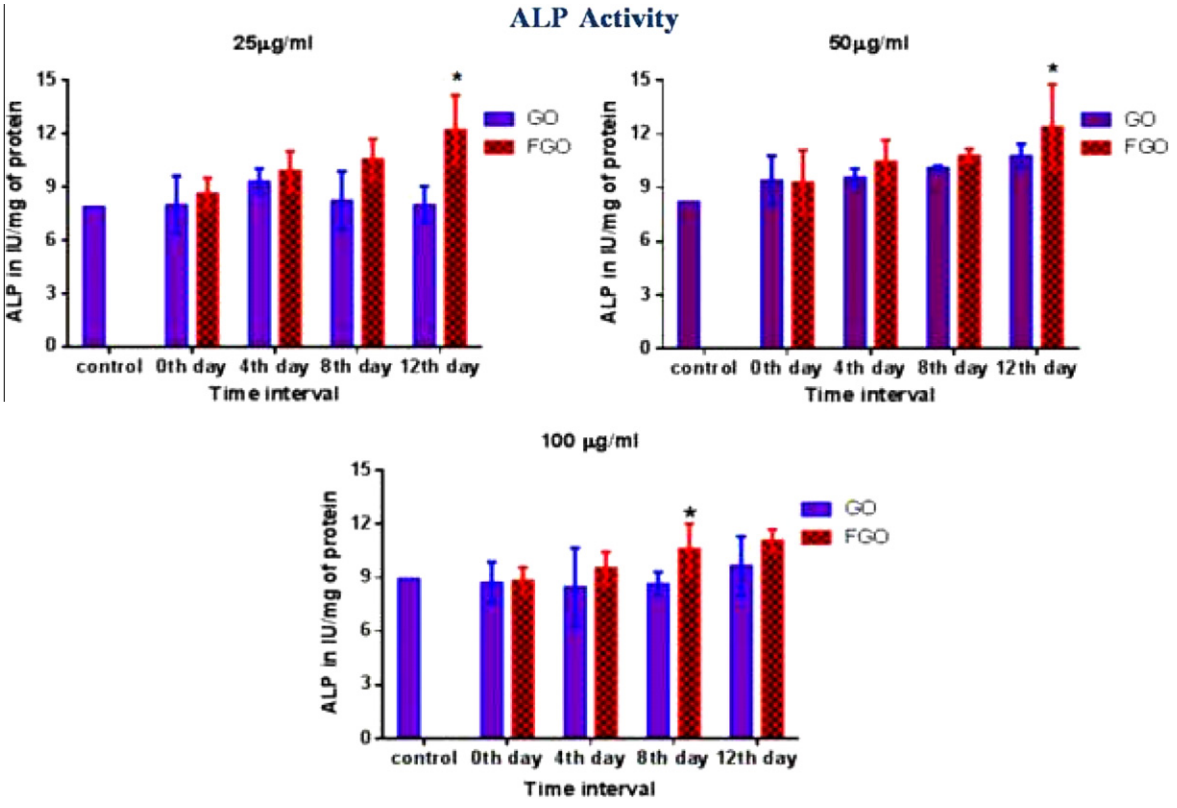

Fig. 10 – ALP representation of MG-63 by the treatment of GO, FGO up to 12 days. Significant difference ($p \leqslant 0.05$) occurred at the 12th day of FGO (25, 50 µg/ml), 8th day of FGO (100 µg/ml). The significant difference was calculated by using t-test.

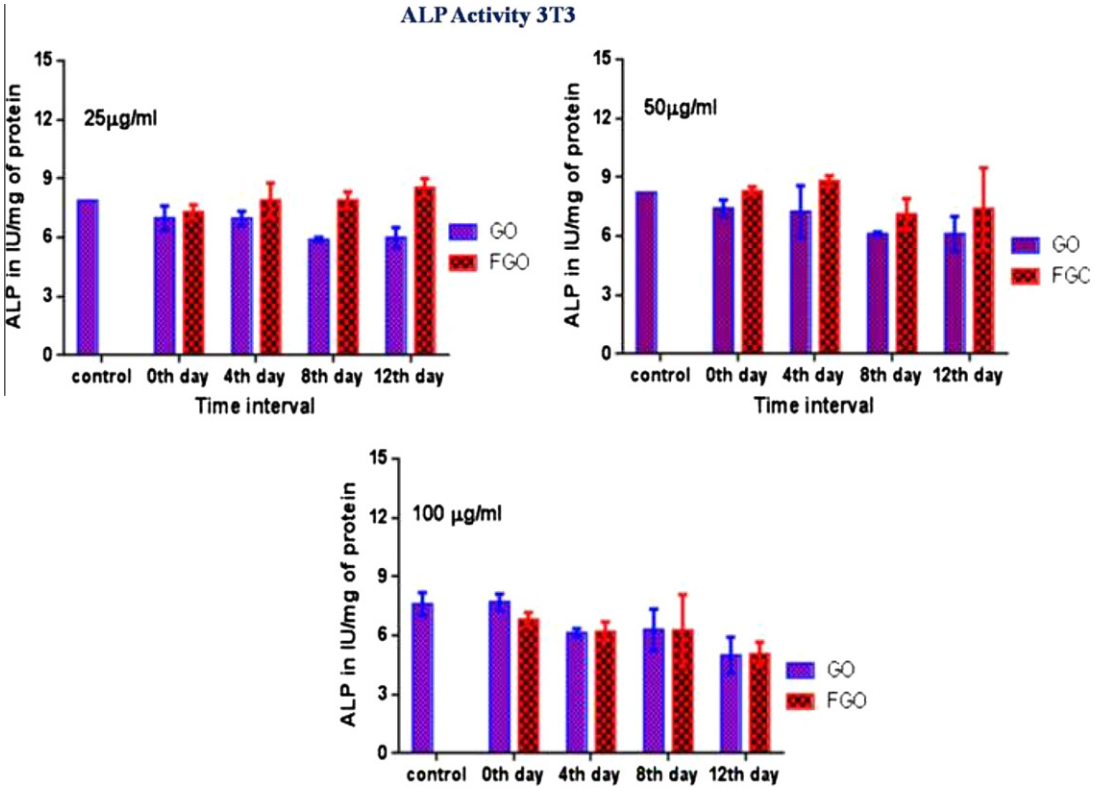

Fig. 11 – ALP representation of NIH 3T3 by the treatment of GO, FGO up to 12 days. There is no any significance difference has occurred. The significance difference was calculated by using *t*-test.

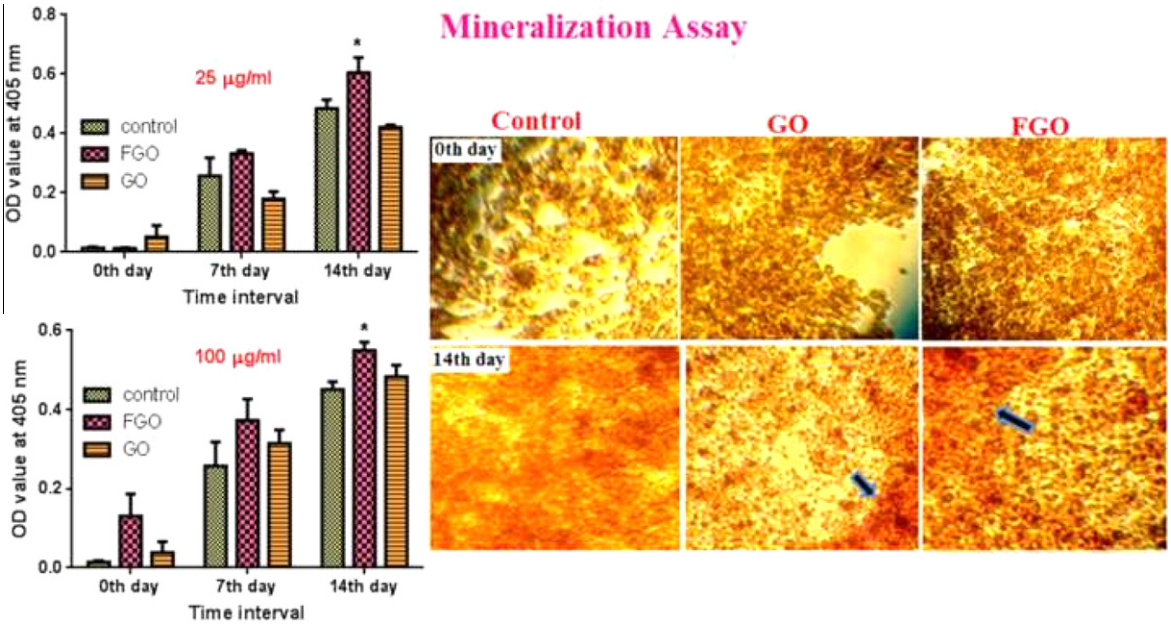

Fig. 12 – Alizarin Red Assay test for GO, FGO on MG-63 up to 14 days. The significant difference ($p \leqslant 0.05$) is occurred at 14th day of FGO (25, 100 μg/ml). The significant difference was calculated by using *t*-test. The microscopic image shows the stain of the Alizarin red at 0th and 14th day of GO and FGO (100 μg/ml).

The decrease in enzyme activity depends on (a) time (b) mineral deposition and (c) covalent bond formation with enzyme [28]. The long time incubation denatures the enzyme and stops the enzymatic action. The low level concentration of GO may not administrate the mineral deposition on the ALP active site. In our study, the main factor which might

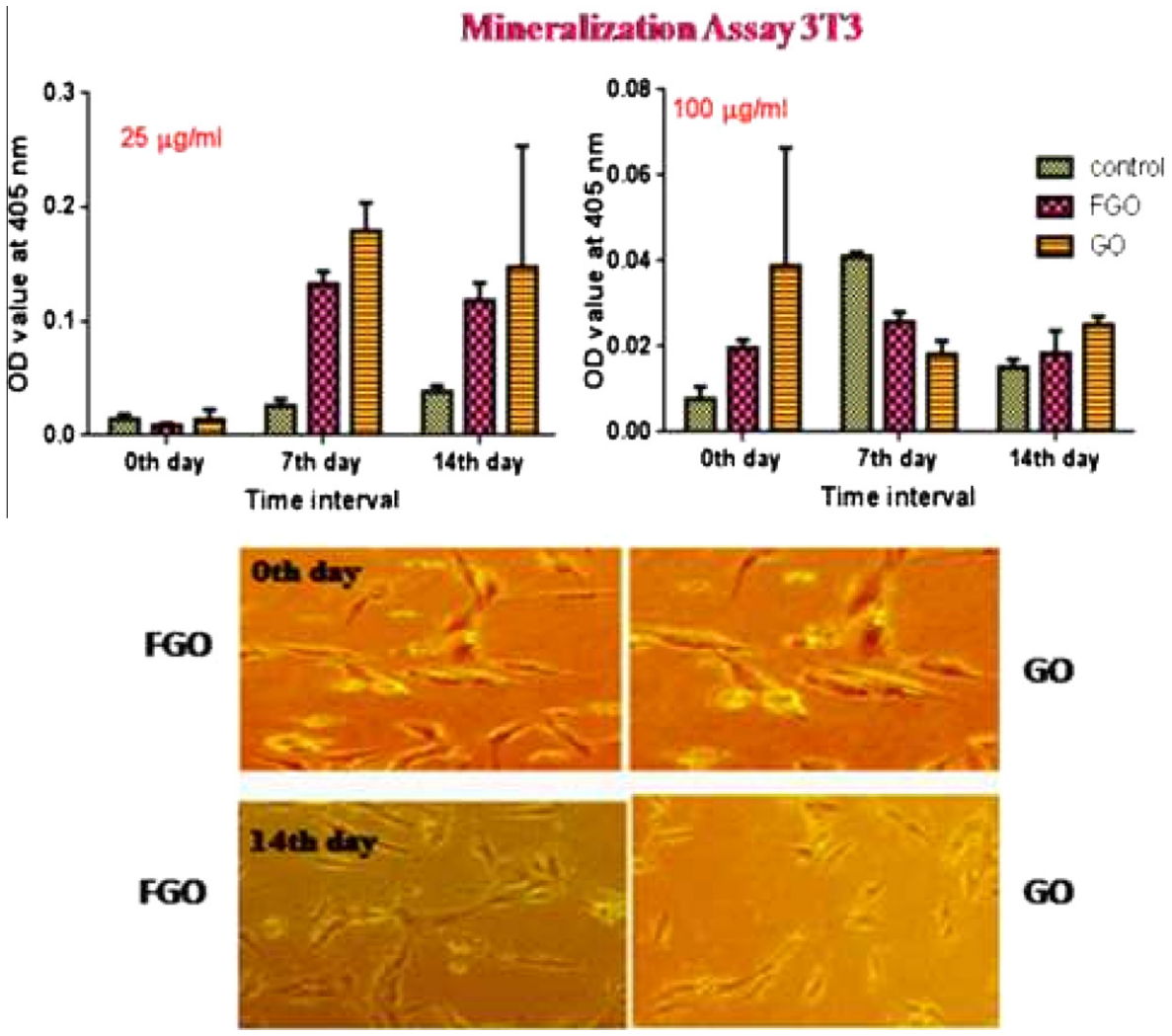

Fig. 13 – Alizarin Red Assay test for GO, FGO on NIH 3T3 up to 14 days. There is no any significant difference ($p \leqslant 0.05$) has occurred. The significant difference was calculated by using *t*-test. The microscopic image shows the stain of the Alizarin red at 0th and 14th day of GO and FGO (100 μg/ml).

be responsible for the decreased level of enzymatic activities is the polar group present in the GO would have formed the covalent bond with ALP enzyme.

Mineralization was measured by the deposition of calcium ions in the cells. Calcium and phosphate distribution are the important factors for the osteognesis [39]. The alizarin red-S (ARS) determines the amount of calcium mineral deposition. The calcium assay results were given as the OD values of ARS extracted from the stained culture of MG-63(Fig. 12) and NIH 3T3 (Fig. 13) cells. The intensity level of Ca^{2+} ion release is increased from 0th to 14th day. Higher level of OD values were observed on 14th day with 25,100 μg/ml concentration of FGO compared with GO. This result is highly correlated with the ALP activity level. Significant Ca^{2+} level difference occurs at 25,100 μg/ml on 14th day of FGO. When compared to 100 μg/ml, the 25 μg/ml GO has slightly reduced the release of ion on 14th day; these results are in agreeing with the ALP levels.

The inverted microscopic image shows the ARS staining after the treatment of GO and FGO on cells. In this image calcium deposition is indicated by the red color, the 100 μg/ml at 14th day shows the maximum deposition of calcium staining. The biocompatibility, ALP and mineralization for the 100 μg/ml were highly associated with cell proliferation, cell attachment, cell differentiation and osteoinduction effect of FGO on MG-63 and were not observed in NIH 3T3 cells.

4. Summary

This preliminary study has shown that fibrin decorated graphene oxide (FGO) has exhibited enhanced osteoinductive properties with good biocompatibility. These properties were proved by MTT assay, ALP activation and Calcium ion release in *in vitro*. Based on these results it was concluded that FGO might be tried as a scaffold in bone tissue engineering applications. The disadvantage of using GO may be non-uniformity in size and shape of its particles and this size variation may hamper the transfection of nanocomposite into the cells.

Acknowledgments

We gratefully acknowledge the financial support provided by Department of Science and Technology (DST).

REFERENCES

[1] Geim AK, Novoselov KS. The rise of graphene. Nat Mater 2007;6:183–91.
[2] Mohanty N, Berry V. Graphene-based single-bacterium resolution biodevice and dna transistor: interfacing graphene derivatives with nanoscale and microscale biocomponents. Nano Lett 2008;8(12):4469–76.
[3] Fan HL, Wang LL, Zhao KK, Li N, Shi Z, Ge Z, et al. Fabrication, mechanical properties, and biocompatibility of graphene-reinforced chi-tosan composites. Biomacromolecules 2010;11(9):2345–51.
[4] Liu Z, Robinson JT, Sun X, Dai H. PEGylated nano-graphene oxide for delivery of water insoluble cancer drugs. J Am Chem Soc 2008;130(33):10876–7.
[5] Zhao X, Zhang Q, Hao Y, Li Y, Fang Y, Chen D. Alternate multilayer films of poly(vinyl alcohol) and exfoliated graphene oxide fabricated via a facial layer-by-layer assembly. Macromolecules 2010;43(22):9411–6.
[6] Lee WC, Lim CH, Shi H, Tang LA, Wang Y, Lim CT, et al. Origin of enhanced stem cell growth and differentiation on graphene and graphene oxide. ACS Nano 2011;5(9):7334–41.
[7] Wang Y, Li Z, Wang J, Li J, Lin Y. Graphene and graphene oxide: biofunctionalization and applications in biotechnology. Trends Biotechnol 2011;29(5):205–12.
[8] Allen MJ, Tung VC, Kaner RB. Honeycomb carbon: a review of graphene. Chem Rev 2010;110(1):132–45.
[9] Bensaid W, Triffitt JT, Blanchat C, Oudina K, Sedel L, Petite H. A biodegradable fibrin scaffold for mesenchymal stem cell transplantation. Biomaterials 2003;24(14):2497–502.
[10] Ye Q, Zund G, Benedikt P, Jockenhoevel S, Hoerstrup SP, Sakyama S, et al. Fibrin gel as a three dimensional matrix in cardiovascular tissue engineering. Eur J Cardiothorac Surg 2000;17(5):587–91.
[11] Rowe SL, Lee S, Stegemann JP. Influence of thrombin concentration on the mechanical and morphological properties of cell-seeded fibrin hydrogels. Acta Biomater 2007;3(1):59–67.
[12] Noorjahan SE, Sastry TP. Physiologically clotted fibrin-calcined bone composite-a possible bone graft substitute. J Biomed Mater 2005;75(2):343–50.
[13] Sastry TP, Rose C, Gomathinayagam S, Ganga R. Chemically modified fibrin–gelatin composites: preparation and characterization. J Appl Pol Sci 1998;68(7):1109–15.
[14] Bosch P, Braun F, Eschberger J, Kovac W, Spängler HP. The action of high-concentrated fibrin on bone healing. Arch Orthop Unfallchir 1977;89(3):259–73.
[15] Homminga GN, Buma P, Koot HW, van der Kraan PM, van den Berg WB. Chondrocyte behaviour in fibrin glue in vitro. Acta Orthop Scand 1993;64(4):441–5.
[16] Kania RE, Meunier A, Hamadouche M, Sedel L, Petite H. Addition of fibrin sealant to ceramic promotes bone repair:long-term study in rabbit femoral defect model. J Biomed Mater Res 1998;43(1):38–45.
[17] Abiraman S, Varma HK, Umashankar PR, John A. Fibrin glue as an osteoinductive protein in a mouse model. Biomaterials 2002;23(14):3023–31.
[18] Fang H, Peng S, Chen A, Li F, Ren K, Hu N. Biocompatibility studies on fibrin glue cultured with bone marrow mesenchymal stem cells in vitro. J Huazhong Univ Sci Technolog Med Sci 2004;24(3):272–4.
[19] Vandrovcova M, Bacakova L. Adhesion, growth and differnation of osteoblasts on suface modified materials developed for bone implants. Physiol Res 2011;60(3):403–17.
[20] Hummers WS, Offeman RE. Preparation of graphitic oxide. J Am Chem Soc 1958;80(6). 1339–1339.
[21] Pacheco-Pantoja EL, Ranganath LR, Gallagher JA, Wilson PJ, Fraser WD. Receptors and effects of gut hormones in three osteoblastic cell lines. BMC Physiol 2011;11:1–14.
[22] Gregory CA, Gunn WG, Peister A, Prockop DJ. An Alizarin red-based assay mineralization by adherent cells in culture: comparison with cetylpyridinium chloride extraction. Anal Biochem 2004;329(1):77–84.
[23] Shen J, Yan B, Shi M, Ma H, Li N, Ye M. Synthesis of graphene oxide-based biocomposites through diimide-activated amidation. J Colloid Interf Sci 2011;356(2):543–9.
[24] Liao K-H, Lin Y-S, Macosko CW, Haynes CL. Cytotoxicity of graphene oxide and graphene in human erythrocytes and skin fibroblasts. ACS Appl Mater Interfaces 2011;3(7):2607–15.
[25] Xue L, Shen C, Zheng M, Lu H, Li N, Ji G, et al. Hydrothermal synthesis of graphene–ZnS quantum dot nanocomposites. Mater Lett 2011;65(2):198–200.
[26] Depan D, Girase B, Shah JS, Misra RD. Structure–process–property relationship of the polar graphene oxide-mediate cellular response and stimulated growth of osteoblasts on hybrid chitosan network structure nanocomposite scaffolds. Acta Biomater 2012;7(9):3432–45.
[27] Sathian J, Sastry TP, Suguna L, Lakshminarayana Y, Radhakrishnan G. Fibrin as a matrix for grafting 2-hydroxyethyl methacrylate: preparation and characterization of the graft and its in vivo evaluation for wound healing. J Biomed Mater Res A 2003;65(4):435–40.
[28] Osathanon T, Giachelli CM, Somerman MJ. Immobilization of alkaline phosphatase on microporous nanofibrous fibrin scaffolds for bone tissue engineering. Biomaterials 2009;30(27):4513–21.
[29] Kalbacova M, Broz A, Kong J, Kalbac M. Graphene substrated promote adherence of human osteoblasts and mesenchymal stromal cells. Carbon 2010;48(15):4323–9.
[30] Bacakova L, Walachova K, Svorcik V, Hnatowicz V. Adhesion and proliferation of rat vascular smooth muscle cells (VSMC) on polyethylene implanted with O+ and C+ ions. J Biomater Sci Polym Ed 2001;12(7):817–34.
[31] Sasidharan A, Panchakarla LS, Chandran P, Menon D, Nair S, Rao CN, et al. Differntial nano-bio interactions and toxicity effects of pristine versus functionalized graphene. Nanoscale 2011;3(6):2461–4.
[32] Wojtoniszak M, Chen X, Kalenczuk RJ, Wajda A, Qapczuk J, Kurzewski M, et al. Synthesis, dispersion, and cytocompatibility of graphene oxide and reduced graphene oxide. Colloids Surf B Biointerfaces 2012;89:79–85.
[33] Lu CH, Zhu CL, Li J, Liu JJ, Chen X, Yang HH. Using graphene to protect DNA from cleavage during cellular delivery. Chem Commun 2010;46(18):3116–8.
[34] Wang K, Ruan J, Song H, Zhang JL, Wo Y, Guo SW, et al. Biocompatibility of graphene oxide. Nanoscale Res Lett 2011;6:1–8.
[35] Chang Y, Yang ST, Liu JH, Dong E, Wang Y, Cao A, et al. In vitro toxicity evaluation of graphene oxide on A549 cells. Toxicol Lett 2011;200(3):201–10.
[36] Zhang Y, Nayak TR, Hong H, Cai W. Graphene: a versatile nanoplatform for biomedical applications. Nanoscale 2012;4(13):3833–42.

[37] Nayak TR, Andersen H, Makam VS, Khaw C, Bae S, Xu X, et al. Graphene for controlled and accelerated osteogenic differentiation of human mesenchymal stem cells. ACS Nano 2011;5(6):4670–8.

[39] Yuan H, Yang Z, Li Y, Zhang X, De Bruijn JD, De Groot K. Osteinduction by calcium phosphate biomaterials. J Master Sci Master Med 1998;9(12):723–6.